2004

A Numerical Study of the Hampson-Type Joule-Thomson Cooler

Hui Tong Chua
National University of Singapore

Xiao Lin Wang
National University of Singapore

Hwee Yean Teo
National University of Singapore

Kim Choon Ng
National University of Singapore

A NUMERICAL STUDY OF THE HAMPSON-TYPE JOULE-THOMSON COOLER

Hui Tong CHUA[1+], Xiaolin WANG[1*], Hwee Yean TEO[2] and Kim Choon NG[1++]

[1] Department of Mechanical Engineering, National University of Singapore, 10 Kent Ridge Crescent, Singapore 119260, Singapore. Tel no.: (65)68746627, Fax no.: (65)67791459,
E-mail id: [+]mpecht@nus.edu.sg, * mpewx@nus.edu.sg, [++] mpengkc@nus.edu.sg

[2] Office of Estate & Development, National University of Singapore, 2 Estate Office Drive, Singapore 117587,
E-mail id: oedthy@nus.edu.sg

ABSTRACT

Miniature Joule-Thomson (J-T) cooler is widely used in the electronic industry for thermal management of power intensive electronic components due to its special features of having a short cool-down time, simple configuration and having no moving parts. In this paper, the sophisticated geometry of the Hampson-type J-T cooler is analyzed and incorporated into the simulation, so that the model is a useful design tool. The governing equations of the cryogen, helical tube and fins, and shield are coupled and solved numerically under the steady state conditions, and yield agreements with experiment data to within 3%. The characteristics of flow within the capillary tube and external return gas are accurately predicted. The temperature versus entropy, cooling capacity versus load temperature, and cooling capacity versus input pressure charts are plotted and discussed. The conventional way of simulating a Hampson-type J-T cooler, which is accompanied by a host of empirical correction factors, especially vis-à-vis the heat exchanger geometry could now be superseded. The effort and time spent in designing a Hampson-type J-T crycooler could be greatly reduced.

1. INTRODUCTION

The miniature Joule-Thomson (J-T) cryocooler has been a popular technology in the electronic industry. It is widely used for rapid cooling of infrared sensors and electronics devices due to its special features of having a short cool-down time, simple configuration and having no moving parts (Aubon, 1988, Joo et al. 1995, Levenduski et al. 1996). Fig.1 shows a typical Hampson-type cryocooler. The cooling power is generated by the isenthalpic expansion of a high pressure gas through a throttling (capillary) device, or namely the Joule-Thomson (J-T) effect. The performance of this cooler is amplified and improved by using the recuperative effect of the expanded gas to pre-cool the incoming stream inside the capillary tube in a counter-flow heat exchanging arrangement.

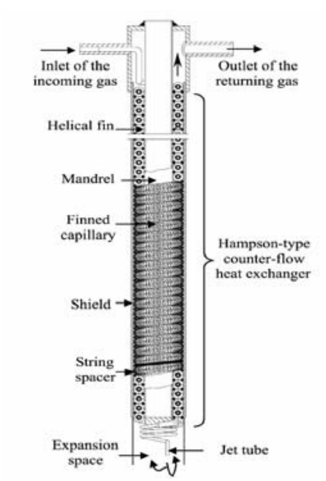

Fig.1a A Hampson-type J-T cryocooler (Xue, 2001)

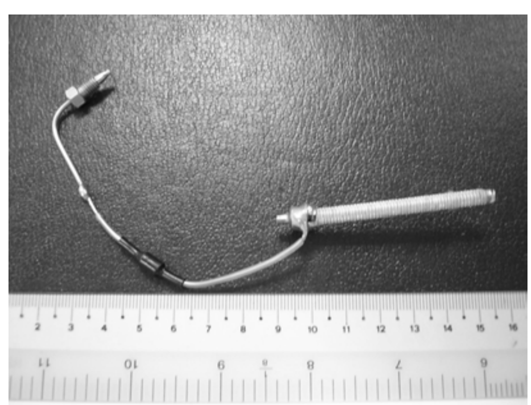

Fig.1b A picture of the Hampson-type J-T cryocooler

Numerical studies on the J-T coolers have hitherto been focusing on the prediction of cool-down rates albeit with an extensive use of empirical correction factors for the heat exchanging geometry. There are limited experimental and theoretical works reported on the prediction of the flow characteristics for the Hampson-type Joule-Thomson (J-T) cooler. Maytal (1994) analyzed the performance of an ideal flow regulated Hampson-type Joule-Thomson (J-T) cooler. The prediction was not realistic because the heat-and-mass transfers among the cryogen, tube wall, Dewar and mandrel were not considered. Chou et al. (1993, 1995) performed experiments and preliminary numerical predictions on the transient characteristics of a Hampson-type Joule-Thomson (J-T) cooler. A one-dimensional model incorporating momentum and energy transport equations was presented. However, secondary flow, torsion effect caused by the helical capillary tube and fins, and the choking of flow were not considered. Idealized heat transfer coefficients of the tube wall, Dewar and mandrel were used in the simulation. This is not true as the heat transfer coefficient varies significantly with the temperature. Chien et al. (1996) simulated the transient characteristics of a self-regulating Hampson-type Joule-Thomson (J-T) cooler. However, this paper concentrated primarily on the development of the self-regulating Hampson-type Joule-Thomson (J-T) cooler by bellows control mechanism. The simulation approach was similar to that of Chou et al. (1995). Recently, Ng et al. (2002) simulated the performance of a Hampson-type Joule-Thomson (J-T) cooler on its effectiveness, flow characteristics, heat conduction and liquefied yield fraction. Again, the torsion, secondary flow effect, and the choking of flow were not considered. Straight tube and straight fins were used in the simulation despite the fact that it was a Hampson-type heat exchanger. Furthermore, their formulation exhibits significant thermodynamic inconsistency.

In this paper, the sophisticated geometry of the Hampson-type heat exchanger is analyzed and incorporated into the model. The characteristics of high pressure gas, return gas, the mandrel, capillary tubes and fins are numerically simulated. The choking of flow in the capillary tube is also considered. The performance of the Hampson-type Joule-Thomson (J-T) cooler in steady state condition is accurately predicted. The conventional way of simulating the Hampson-type Joule-Thomson cooler, which is accompanied by a host of empirical correction factors, especially vis-à-vis the heat exchanger geometry could now be superseded. The effort and time spent in designing a Hampson-type Joule-Thomson (J-T) cooler could be greatly reduced. Since we have totally avoided the use of empirical geometric correction factors, the model is a very helpful design tool.

2. THERMODYNAMIC MODEL

The performance of a Hampson-type Joule-Thomson (J-T) cooler could be determined if the amount of energy transfer among the high pressure gas, tube wall, fins and return gas at any instant is evaluated. The helical geometry of the capillary tube and fins are analyzed and solved together with the governing equations. The governing equations for the energy balance, conservation of mass, the thermal conduction and radiation are discretized, coupled and simulated numerically. These governing equations are listed in the following sections.

2.1. High Pressure Gas in the Helical Capillary Tube

Since the capillary tube diameter is much smaller compared to the capillary tube length, approximately 1 to 1840, one-dimension steady state flow is assumed. The conservation of mass of the high pressure gas inside the helical capillary tube could be expressed as,

$$\frac{d\dot{m}_f}{ds} = 0 \tag{1}$$

The pressure inside the capillary tube drops rapidly due to the high velocity of the flow and viscosity of the gas. The one-dimensional pressure drop along the natural helical direction (or the s-direction) of the capillary tube is given by,

$$\frac{dp_f}{ds} = -\frac{2f_f\rho_f u_f^2}{D_{mi}} - \frac{d(\rho_f u_f^2)}{ds} \tag{2}$$

where f_f is the Fanning friction factor of the high pressure gas. Timmerhaus and Flynn (1989) suggested an empirical expression for f_f for the gas flow in a helical tube as,

$$f_f(p_f, T_f) = 0.184(1.0 + 3.5\frac{D_{mi}}{D_{Hx}})Re(p_f, T_f)^{-0.2} \tag{3}$$

The temperature of the high pressure gas varies along the capillary tube due to the drop of pressure, frictional loss and heat transfer between the gas and the tube wall. It is expressed as,

$$h_f(T_m - T_f)\pi D_{mi} = G_f A_f \left[c_{pf}\frac{dT_f}{ds} + \left(v_f - T_f \frac{\partial v_f}{\partial T_f} \right)\frac{dp_f}{ds} + \frac{d(u_f^2/2)}{ds} \right] \tag{4}$$

where the heat transfer coefficient, h_f, could be expressed as,

$$h_f = 0.023 c_p G_f \, Re^{-0.2} \, Pr^{-2/3}(1.0 + 3.5\frac{D_{mo}}{D_{Hx}}) \tag{5}$$

2.2. Helical Capillary Tube

The energy balance equation in the helical capillary tube is,

$$\frac{d^2T_m}{ds^2} = -\frac{h_f(T_m - T_f)(A_{fm}/ds)}{A_m k_m} - \frac{h_l(T_m - T_l)(A_{ml}/ds)}{A_m k_m} - \frac{2k_T(T_m - T_{fin})(A_{finm}/ds)}{A_m k_m} \tag{6}$$

where
$$k_T = \frac{k_m \cdot k_{fin}}{k_{fin} \cdot W_{fin} + k_m \cdot H_{fin}} \tag{7}$$

2.3. Helical Fins

The energy balance equation for the helical fins wound around the helical capillary tube can be expressed as,

$$\frac{d^2T_{fin}}{ds^2} = -\frac{h_l(T_{fin} - T_l)(A_{finl}/ds)}{A_{fin} k_{fin}} - \frac{2k_T(T_{fin} - T_m)(A_{finm}/ds)}{A_{fin} k_{fin}} \tag{8}$$

2.4. Shield

The energy balance equation for the shield could be written as,

$$\frac{d^2T_{sh}}{dz^2} = -\frac{h_l(T_{sh} - T_l)\pi D_{si}}{A_{si} k_{sh}} - \frac{h_r \pi D_{si}(T_{sh}^4 - T_{amb}^4)}{A_{si} k_{sh}} \tag{9}$$

where h_r is the radiative heat transfer coefficient given by,

$$h_r = \frac{\sigma}{1/\varepsilon_{sh} + (A_{sh}/A_r)(1/\varepsilon_r - 1)} \tag{10}$$

2.5. Return Gas

The conservation of mass and momentum equations of the return gas along the primary axial direction (or the z-direction) of the helical capillary tube and fins could be expressed as,

$$\frac{d\dot{m}_l}{dz} = 0 \tag{11}$$

$$\frac{dp_l}{dz} = \frac{2 f_l \rho_l u_l^2}{D_{Hl}} + \frac{d(\rho_l u_l^2)}{dz} \tag{12}$$

where f_l is the Fanning friction factor of the return low pressure gas and it is written as,

$$f_l(p_l, T_l) = 0.184 \, Re(p_l, T_l)^{-0.2} \tag{13}$$

The energy balance equation of the return gas along the primary axial direction (or the z-direction) of the heat exchanger is given by,

$$h_l(T_l - T_m)\frac{A_{ml}}{dz} + h_l(T_l - T_{fin})\frac{A_{finl}}{dz} + h_l(T_l - T_{sh})\pi D_{shi} = G_l A_l \left[c_{pl}\frac{dT_l}{dz} + \left(v_l - T_l \frac{dv_l}{dT_l} \right)\frac{dp_l}{dz} + \frac{d(u_l^2/2)}{dz} \right] \tag{14}$$

where the heat transfer coefficient, h_l could be expressed as,

$$h_l = 0.26 c_p G_l \, Re^{-0.4} \, Pr^{-2/3} \tag{15}$$

The conversion factor between *ds* and *dz* is given by,

$$\frac{ds}{dz} = \frac{\sqrt{(Pitch_m/2\pi)^2 + R_{curve}^2}}{Pitch_m \,/\, 2\pi} \tag{16}$$

2.6. Spacers

Nylon strings, which possess an extremely low thermal conductivity, is used to wind round the helical capillary tube and fins, so as to limit the cross-sectional area available to the returning low pressure gas and thereby enhancing its contact with the fins and the primary helical capillary tube. In our model, we assume that the spacers play the sole role of limiting the heat exchange cross-sectional area.

2.7. Entropy Generation for High Pressure Gas in the Helical Capillary Tube

The entropy generation equation is used to assess the choking position of the high pressure gas in the capillary tube and is expressed as,

$$\frac{dS_{gen}}{ds} = \dot{m}_f \left\{ \frac{1}{T_f}\left[c_{pf}\frac{dT_f}{ds} + \left(\frac{1}{\rho_f} + \frac{T_f}{\rho_f^2}\frac{d\rho_f}{dT_f} \right)\frac{dp_f}{ds} \right] - \frac{1}{\rho_f T_f}\frac{dp_f}{ds} \right\} - h_f\left(\frac{T_m - T_f}{T_m} \right)\cdot\frac{A_{fm}}{ds} \tag{17}$$

2.8. Thermo-physical Properties of the Cryogen and Materials

In this context, argon is chosen as the cryogen due to its easy availability, low cost and being able to achieve relatively low cryogenic temperature. The thermo-physical properties of argon are obtained from the software of NIST (2001) which makes use of the Helmhotz energy equation, a modified Benedic-Webb-Rubin equation (mBWR), and an extended corresponding states model (ECS). The viscosity and thermal conductivity values are determined with a fluid specific model and a variation of the ECS method.

Temperature-dependent thermal conductivities of copper, monel, stainless steel and polycarbonate are used in the simulation. The polycarbonate could be readily substituted by the Dewar in actual applications. Copper is used for the fins that are wound round the stainless steel capillary tube. The assembly is inserted into the shield, which is made of monel, and insulated with polycarbonate. The exterior of the polycarbonate is assumed to be perfectly insulated in our model. The relevant empirical correlations are summarized in Table 1 (Perry et al., 1997 and Flynn, 1997).

Table 1 Thermal conductivities of materials

Materials	Correlation	Relative Errors (Perry,1997)
Copper (Fins)	$k_{fin} = \{ \begin{array}{l} 0.2413T^2 - 47.775T + 2848, (60K \le T \le 100K) \\ 0.028T^2 - 1.525T + 608, (100K \le T \le 300K) \end{array}$	< 1.5%
Monel (Shield)	$k_{sh} = 6.5169 \ln T - 14.76, (40K \le T \le 400K)$	< 1.0%
Stainless Steel (Capillary Tube)	$k_m = 5.0353 \ln T - 13.797, (40K \le T \le 400K)$	< 1.0%

2.9. Jet Impingement Boiling

The jet impingement boiling correlation on the heated surface proposed by Brian (1991) is used to estimate the heat flux at the load.

$$Q/A = 181.1463 \left(\Delta T\right)^{1.218}$$

where ΔT is the temperature difference between the surface and the measured bulk fluid.

3. RESULTS AND DISCUSSION

Our simulation is applied to a Hampson type J-T cooler which is shown in the figure 1b. The dimensions of the Hampson-type Joule-Thomson (J-T) cooler are listed in the table 2.

Table 2: Typical dimensions of a Hampson-type Joule-Thomson (J-T) heat exchanger

Items	Inner diameter, mm	Outer diameter, mm
Capillary tube, helical pitch = 1.0 mm	0.3	0.5
Mandrel	2.3	2.5
Shield	4.5	4.8
Fins: height = 0.5 mm, thickness = 1.0 mm, secondary pitch = 0.25 mm		
Length of heat exchanger = 50.0 mm		

The simulation results are compared with the experimental data as shown in table 3. Only the relative errors of the outlet temperatures of the return gas are compared with the simulated results. This is due to the unavailability of tiny sensors to measure the pressure and temperature in the capillary tube. It is noted that the measured return gas outlet temperature is slightly higher than the simulated results. This could be due to:

i. the use of the polycarbonate instead of a Dewar flask, which inevitably increases the heat gain during the experiment.
ii. readings of the temperature sensor at the return gas outlet are affected by the ambient conditions, on account of the minuteness of the exit port.

However, it is observed that the relative errors between the simulations and experiments all fell within 3%.

Table 4. A comparison between the experimental data and simulation results

Case	Pressure (bar)		Temperature (K)		M_v	Temperature (T_{outlet}, K)		Relative
	p_1	p_3	T_{inlet}	$T_{sat}=f(p_3)$	(SLPM)	Experiment	Simulation	Error, %
1	179.12	1.7272	291.49	92.68	13.927	282.57	276.93	2.00
2	169.86	1.7460	291.40	92.80	13.102	283.73	277.12	2.33
3	160.10	1.6362	292.25	92.11	*12.060**	284.77	278.53	2.19
4	149.66	1.4713	292.14	90.99	10.948	284.90	279.20	2.00
5	140.47	1.3426	291.94	90.06	10.145	284.98	279.34	1.98

**The originally reported experimental value (11.943 SLPM) was erroneous. Since the experimental mass flow rates behave essentially linearly with the input pressure, the present value is obtained by linear interpolation.*

Figure 2 shows the Temperature-Entropy diagram of the cryogen in the Hampson-type Joule-Thomson (J-T) cooler. The trend is similar to a typical T-S chart in the literature. However, it is found that the pressure drops much more rapidly due to the higher frictional loss and expansion process in the high pressure gas channel than that in the low pressure channel. This in turn increases the cooling capacity of the Hampson-type Joule-Thomson (J-T) cooler and demonstrates the efficiency of the recuperative method in improving the performance of the Hampson-type Joule-Thomson (J-T) cooler substantially.

Figure 3 presents the effect of the load temperature on the cooling capacity. With an increase in the cooling load temperature, the cooling capacity increases greatly. This corroborates with the basic theory commonly used in the traditional air-conditioning and refrigerant systems. It is noted that the cooling capacity is linearly proportional to the load temperature.

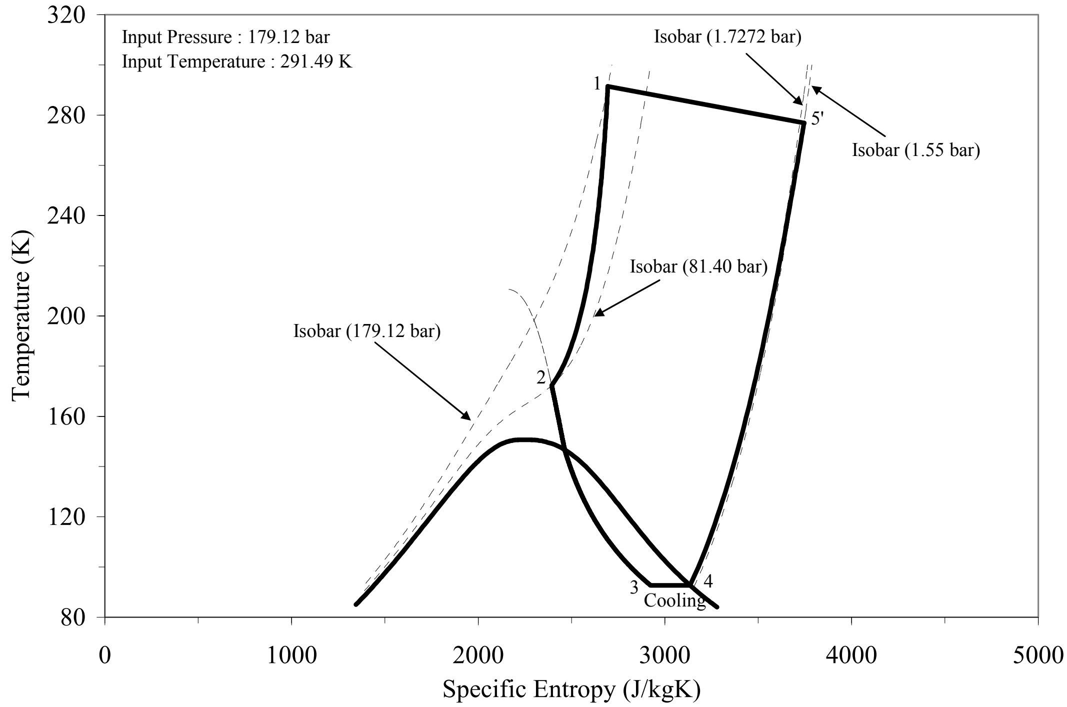

Fig.2 A typical simulated T-s diagram of the Hampson-type Joule-Thomson (J-T) cooler

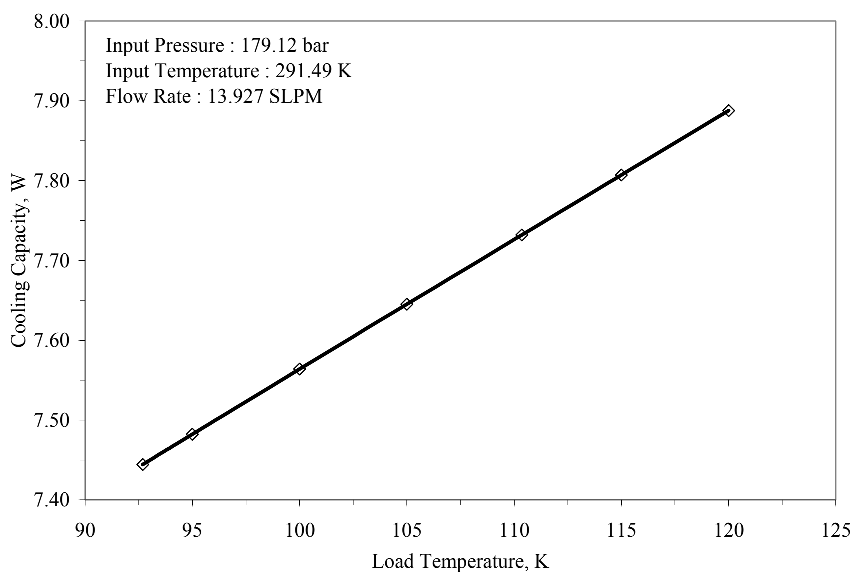

Fig.3 Effect of the load temperature on the cooling capacity

The higher the input pressure, the higher the cooling capacity that could be achieved. This is evident from the simulation results as shown in Fig 4. Within our simulated range, the cooling capacity increases as the input pressure increases. It is observed from the chart that the cooling capacity increases gently at the lower range of pressures while it increases more rapidly at the higher range.

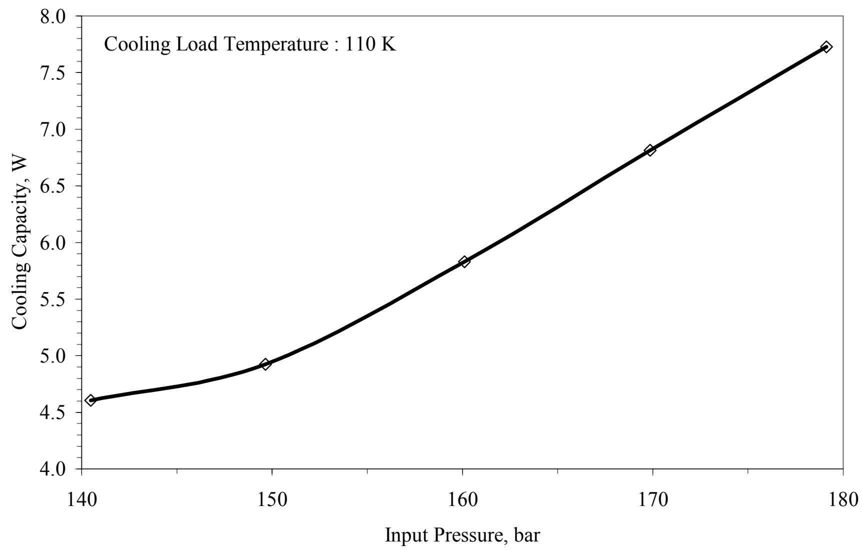

Fig.4 Effect of the input pressure on the cooling capacity

CONCLUSION

A simulation design tool for the Hampson-type Joule-Thomson (J-T) cooler has been developed according to the correct geometry of the helical capillary tube and fins. The result shows that the numerical simulation agrees with the experimental data. The performance characteristics of the Hampson-type Joule-Thomson (J-T) cooler are analyzed and discussed. Therefore, it could be concluded that this simulation is useful for the prediction, estimation and evaluation of the Hampson-type J-T cooler. It provides realistic design solutions for the manufacturers to design a J-T cooler and avoid most of the "trial and error" procedures commonly adopted.

NOMENCLATURE

A	Contact area (m^2)	Superscripts & Subscripts	
c_p	Specific heat capacity (J/kg K)	amb	Ambient
D	Tubes diameter (m)	f	Refrigerant inside the tube
f	Fanning friction coefficient	fin	Capillary fins
G	Mass flux ($kg/m^2.s$)	l	Return refrigerant along the fins
h	Heat transfer coefficient (W/m^2 K)	m	Capillary tube
k	Conductivity (W/m.K)	man	Mandrel
$\dot{m}$	Mass flow rate (kg/s)	mi	Capillary tube interior
p	Pressure (Pa)	min	Minimum
Pr	Prandtl number = $c_p.\mu / k$	mo	Capillary tube exterior
q	Heat flux (W)	out	Outlet
R, r	Radius (m)	sat	Saturation situation
R_{curve}	Radius of curvature of capillary tube	sh	Shield
Re	Reynolds number	si	Shield interior
S_{gen}	Entropy generation (J/K)	Tot	Total
s	J-T primary helical direction (capillary tube)	Hx	Hydraulic diameter
T	Temperature (K)		
u	Bulk mean velocity of cryogen (m/s)		
W,H	Effective width length and Height for fin (m)		
z	J-T primary axial direction		
μ	Viscosity (N s/m^2)		
ρ	Density (kg/m^3)		
σ	Stefan-Boltzmann constant ($W/(m^2.K^4)$)		

REFERENCE

Aubon, C.R., 1998, Joule-Thomson Cooling-An Overview, *SPIE*, vol. 915, p. 32-33.

Brian, A., Sherman, S., Schwartz, H., 1991, Jet Impingement Boiling Using a J-T Cryostat, *Cryogenic Heat Transfer* vol. 167, p. 11-17.

Chien, S.B., Chen, L.T., Chou, F.C., 1996, A study on the Transient Characteristics of a Self-regulating Joule-Thomson Cryocooler, *Cryogenics*, vol. 36, p. 979-984.

Chou, F.C., Wu, S.M., Pai, C.F., 1993, Prediction of Final Temperature Following Joule-Thomson Expansion of Nitrogen Gas, *Cryogenics*, vol. 33, p. 857-862.

Chou, F.C., Chien, S.B., 1995, Preliminary Experimental and Numerical Study of Transient Characteristics for a Joule-Thomson Cryocooler, *Cryogenics,* vol. 35, p. 311-316.

Flynn, M.T., 1997, *Cryogenic engineering*, Marcel Dekker Inc., NewYork.

Joo, Y., Dieu, K., Kim, C., 1995, Fabrication of Monolithic Microchannels for IC chip cooling, *IEEE*, p. 362-367.

Lemmon, E.W., Peskin, A.P., McLinden, M.O., Friend, D.G., 2000, Thermodynamic and transport properties of pure fluids, *NIST Standard Reference Database 12*, Version 5.0

Levenduski, R., Scarlotti, R., 1996, Joule-Thomson Cryocooler for Space Applications, Cryogenics, vol. 36, p. 859-866.

Maytal, B.Z., 1994, Performance of Ideal Flow Regulated Joule-Thomson Cryocooler, *Cryogenics*, vol. 34, p. 723-726.

Ng, K.C., Xue, H., Wang, J.B., 2002, Experimental and Numerical Study on a Miniature Joule-Thomson Cooler for Steady-state Characteristics, *Int. J. Heat & Mass Trans.*, vol. 45, p. 609-618

Timmerhaus, K.D., Flynn, T.M., 1989, *Cryogenic Process Engineering*., Plenum Press, New York, USA.

Xue. H., Ng, K.C., Wang, J.B., 2001, Performance Evaluation of the Recuperative Heat Exchanger in a Miniature Joule-Thomson Cooler, *App. Thermal Eng.*, vol. 21, p. 1829-1844

ACKNOWLEDGEMENT

We gratefully acknowledge the generous support from A*STAR SERC via the project number 0221010035.